Available online at www.sciencedirect.com
ScienceDirect
Zoology 112 (2009) 393–402
ZOOLOGY
www.elsevier.de/zool

# Whole-body lift and ground effect during pectoral fin locomotion in the northern spearnose poacher (*Agonopsis vulsa*)

Bryan N. Nowroozi[a,*], James A. Strother[b], Jaquan M. Horton[c,1], Adam P. Summers[c,1], Elizabeth L. Brainerd[a]

[a]*Department of Ecology and Evolutionary Biology, Brown University, 80 Waterman St., Providence, RI 02912, USA*
[b]*Department of Ecology and Evolutionary Biology, University of California, Irvine, CA 92697, USA*
[c]*Friday Harbor Laboratories, University of Washington, Friday Harbor, WA 98250, USA*

Received 24 April 2008; received in revised form 22 September 2008; accepted 21 November 2008

## Abstract

The northern spearnose poacher, *Agonopsis vulsa*, is a benthic, heavily armored fish that swims primarily using pectoral fins. High-speed kinematics, whole-body lift measurements, and flow visualization were used to study how *A. vulsa* overcomes substantial negative buoyancy while generating forward thrust. Kinematics for five freely swimming poachers indicate that individuals tend to swim near the bottom (within 1 cm) with a consistently small (less than 1°) pitch angle of the body. When the poachers swam more than 1 cm above the bottom, however, body pitch angles were higher and varied inversely with speed, suggesting that lift may help overcome negative buoyancy. To determine the contribution of the body to total lift, fins were removed from euthanized fish ($n = 3$) and the lift and drag from the body were measured in a flume. Lift and drag were found to increase with increasing flow velocity and angle of attack (ANCOVA, $p < 0.0001$ for both effects). Lift force from the body was found to supply approximately half of the force necessary to overcome negative buoyancy when the fish were swimming more than 1 cm above the bottom. Lastly, flow visualization experiments were performed to examine the mechanism of lift generation for near-bottom swimming. A vortex in the wake of the pectoral fins was observed to interact strongly with the substratum when the animals approached the bottom. These flow patterns suggest that, when swimming within 1 cm of the bottom, poachers may use hydrodynamic ground effect to augment lift, thereby counteracting negative buoyancy.


***Keywords:*** Agonidae; Fluid flow; Lift; Locomotion kinematics; Negative buoyancy

## Introduction

Most fishes are only slightly negatively buoyant, but there are both extant and extinct lineages that are heavily armored and benthic in their habit. These fishes often lack the adaptations for neutral buoyancy seen in other fishes, such as a swim bladder or a large positively buoyant liver (Aleev, 1969). Presumably the static sinking force associated with heavy dermal armor has the advantage of more firmly settling the fish on the substrate. The obvious disadvantage to this strategy is clear when the fish moves from one place to another and must overcome this negative buoyancy.

*Corresponding author. Tel./fax: +1 401 863 1032.
*E-mail address:* bryan_nowroozi@brown.edu (B.N. Nowroozi).
[1]Current address: Friday Harbor Laboratories, University of Washington, 620 University Road, Friday Harbor, WA 98250, USA.

0944-2006/$ - see front matter © 2009 Elsevier GmbH. All rights reserved.
doi:10.1016/j.zool.2008.10.005

An example of a lineage with varying degrees of armor, lack of a swim bladder, and association with the bottom is the poachers (Agonidae), of which there are 22 genera with 47 species, all of which are armored to some degree (Nelson, 1994). Fourteen of these species are found in the North Pacific and up to the Arctic, with some species in South America, as well as the North Atlantic. Poachers are particularly interesting because they use only their pectoral fins for propulsion, except during C-start escape responses when the caudal fin is used (personal observation).

Swimming with the pectoral fins, or labriform locomotion, has been well studied and is particularly common in perciform fishes (Breder, 1926; Drucker and Jensen, 1996; Walker and Westneat, 1997, 2001). It is often seen at slower swimming velocities up to a critical swimming speed (Mussi et al., 2002), at which point many fishes transition to a different gait of locomotion in which they use both their caudal and pectoral fins. Pectoral fin locomotion has been categorized into two types: drag-based rowing and lift-based flapping (Blake, 1983). It has been shown that drag-based rowing is a less efficient mode of locomotion than lift-based flapping (Walker and Westneat, 2001). For nearly neutrally buoyant fish swimming in the water column, the pectoral fins deliver not only the thrust that drives the fish forward but also a small excess lift component that offsets negative buoyancy (Drucker and Lauder, 2000).

Here we are interested in the locomotion of a well-armored fish, the northern spearnose poacher, *Agonopsis vulsa*, a benthic species that exclusively employs drag-based pectoral fin propulsion in routine swimming. In addition to being heavily armored, *A. vulsa* lacks a swim bladder, thereby increasing its negative buoyancy. Thus, when not swimming, *A. vulsa* simply sinks to the bottom. Pectoral fin oscillation must provide the thrust to move from place to place since the tail is not used at all, but it is not clear where the lift to offset the relatively high negative buoyancy comes from. Perhaps the pectoral fins are able to generate sufficient excess lift, though it would surely come at the expense of generating thrust. Alternatively, the poacher may be getting significant lift from its body as in sharks and sturgeons, where the body acts as a hydrofoil. These fishes have been shown to increase lift by increasing the angle of attack of the body with respect to flow (Wilga and Lauder, 1999, 2000, 2001).

Benthic species face an additional constraint when generating whole-body lift by manipulating angle of attack. Because they are close to the bottom, they cannot assume high angles without the caudal fin hitting the bottom. However, along with proximity to the bottom comes a potential source of lift that has not yet been explored – that produced through ground effect as pectoral fin-generated vortices make contact with the substrate.

The goals of this study were four-fold: (1) to describe the pectoral fin kinematics of the northern spearnose poacher when swimming close to the bottom and in the water column; (2) to determine the mechanism by which *A. vulsa* is able to counteract its negative buoyancy at different speeds and distances from the bottom; (3) to determine whether there is any interaction between the pectoral fin wake and the bottom; and (4) to measure lift and drag on cadaveric specimens at various angles of attack and flow speeds.

## Materials and methods

Northern spearnose poachers, *A. vulsa*, were collected by trawl at San Juan Island Channel and by beach seine (net) at Jackson Beach, Friday Harbor Island, Washington, USA. Fish were held at the Friday Harbor Laboratories in sea tables with a continuous flow of seawater at a temperature of $13 \pm 1\,^{\circ}C$. Kinematic measurements were made on five adult fish, ranging between 10.1 and 17.5 cm, swimming freely in a still-water aquarium. Total body length (bl) and body mass were measured using electronic calipers and a digital balance, and body volume was measured by displaced volume in water. Effective weights in water were calculated by multiplying average body density by the volume of the fish.

### Kinematics

#### Data collection

Fish were filmed at 1000 frames per second using two MotionScope high-speed video cameras (Redlake Inc., Tallahassee, FL, USA) from lateral and ventral views. The field of view was illuminated using a 100 W Lowel Omni light (Lowel-Light Manufacturing Inc., Brooklyn, NY, USA) and a 650 W halogen lamp. The inner dimensions of the acrylic aquarium were 114 cm × 25 cm with a water depth of 15 cm.

Videos were calibrated by filming a known length in both camera views. This length was taken in the region of the field of view where the fish swam. Calibration videos were taken each time a camera was moved. Scale was then set using Image J (National Institutes of Health, Bethesda, MD, USA) to relate the known length to number of pixels.

Only video sequences in which the fish remained at least 3 cm away from either wall of the aquarium and that captured 2–4 complete pectoral fin beat cycles in both camera views were used for analysis (the remainder were not saved to disk). Video sequences of fish swimming at all heights in the water column were used. A minimum of five acceptable (meeting the criteria above) sequences per individual were collected.

In addition to these quantitative kinematic measurements on five adult *A. vulsa*, qualitative behavioral observations were made of the same five adults plus two juveniles while they were swimming freely in the laboratory sea tables. Observations of swimming behavior were also made on the following species in the sea tables: four-horned poacher (*Hypsagonus quadricornis*), sturgeon poacher (*Agonus acipenserinus*), smooth alligatorfish (*Anaplagonus inermis*), and the blue-spotted poacher (*Xeneretmus triacanthus*).

### Analysis

Image J was used to measure total body velocity ($cm\,s^{-1}$), pectoral fin beat frequency (Hz), average pectoral fin beat amplitude (degrees), and average body pitch angle (degrees) during locomotion for each video sequence. Advance ratios were subsequently calculated.

The distance traveled through the field of view was divided by the duration of frames (in seconds) to generate total body velocities. This distance was measured by following the path of the tip of the fish's nose from the starting frame of video until the last frame where the nose is visible in the field of view. This analysis was performed in the lateral view initially, and verified in the ventral view.

Pectoral fin beat frequency was measured as the inverse of the duration of one representative fin beat cycle per sequence. Pectoral fin beat cycles were defined as starting with the fins fully abducted, adducting towards the body, and then returning to the fully abducted position.

Pectoral fin beat amplitude was measured as the angle, in degrees, between the fully abducted leading edge of the pectoral fin and a longitudinal axis parallel to the body axis of the fish in one representative fin beat per sequence. This longitudinal axis was taken as a straight line from the joint connecting the pectoral fin and the body to the posterior of the fish in the ventral view. This angle was measured at the fully abducted position. It is important to note that this measure of fin beat amplitude is just one component of the true amplitude. The complex pectoral fin stroke of fish contains motion in more than one plane that is not accounted for in the present study (Bozkurttas et al., 2006).

Previous research has shown that advance ratio (*J*-value) is an indicator of mechanical efficiency of the pectoral fin during locomotion (Vogel, 1981; Drucker and Jensen, 1996). The *J*-value is a ratio of total body velocity to pectoral fin tip velocity. This can be calculated by the following equation (Vogel, 1981):

$$J = U/2\phi nR$$

where $U$ is total body velocity, $\phi$ the pectoral fin amplitude, $n$ the pectoral fin beat frequency, and $R$ the length of the fin taken from the insertion on the pectoral girdle to the leading tip of the pectoral fin. The measurements made above were used to calculate the *J*-value with this equation. An analysis of covariance (ANCOVA), with individual and swimming level (categorized as greater than or less than 1 cm above the bottom; high or low) as factors and body velocity as the covariate, was used to determine the effects of swimming velocity and swimming height on advance ratio (JMP version 5.0; SAS Institute, Cary, NC, USA). For all statistical analyses in this study, significance was set at the $p < 0.05$ level.

Body pitch angle (i.e. angle of attack) was measured by drawing a straight line from the nose to the posterior point of attachment of the anal fin, and a horizontal line parallel to the plane of the bottom. The angle between these two lines was used as the pitch angle. This angle was measured with the fins at the fully abducted position. An ANCOVA, with individual and swimming level (high or low) as factors and body velocity as the covariate, was used to determine the effects of swimming velocity and height above the bottom on angle of attack (all statistical analyses in JMP version 5.0).

## Fluid flow visualization

### Data collection

The same still-water aquarium described above was used for imaging fluid flow. The aquarium was thoroughly rinsed with fresh water, and seawater was filtered with a 63-μm sieve. One high-speed video camera (MotionScope PCI 2000S) was used to obtain a lateral view at 125 frames per second. A 5 mW laser was focused into a sheet of light 15 cm in length perpendicular to the lens of the camera. Thus, a two-dimensional visualization of flow was obtained in the present study. An acrylic boat of the dimensions 11.5 cm × 24.8 cm floated above the laser to eliminate turbulent flow and unwanted fluid oscillations at the water surface. Conduct-O-Fil hollow silver microspheres (Potter Industries, Valley Forge, PA, USA) were distributed throughout the aquarium, and were illuminated by the laser to visualize the flow of water. The fish swam through the aquarium in such a way that the distal edge of the pectoral fin passed through the plane of the laser. Videos in which the more proximal portions of the pectoral fin tip passed through the laser were not used. This was done to reduce possible variation in fluid flow resulting from different span-wise portions of the pectoral fin passing through the laser. The stroke of the pectoral fin, as well as the resulting vortices, were then recorded and used for analysis.

### Analysis

Displacements between spherical particles were measured and plotted over 45 frames (0.36 s) to render streaklines. The 45 sequential frames were selected to

begin just after the fish exited the field of view. The streaklines then provided a qualitative visualization of the resultant fluid flow generated by the poacher's fin stroke through water. Flow was visualized for seven swimming events recorded from two fish (10.1 and 16.0 cm, respectively). Both fish were recorded swimming at various heights in the water column and along the bottom of the aquarium.

## Force measurements

### Data collection

To separate the effects of pectoral fin lift and body lift, the pectoral fins were removed postmortem from three euthanized fish (total length 16.0, 16.1, and 17.5 cm; weight in water 19.9, 21.9, 24.0 mN, respectively). The specimens had been previously frozen and were thawed before use. The finless fish were then suspended in a flume by a sting that pierced the lateral body surface of the fish at the longitudinal position of the center of mass (Fig. 1). The sting was constructed as a square, hollow beam with linear pattern strain gages (Vishay Micro-Measurements, Wendell, NC, USA) paired on opposite sides (Fig. 1). Each strain gage was 5.1 mm in length and 3.0 mm in width with a resistance of 120 Ω and a gage factor of 2.065 ± 0.5%. Each pair of strain gages was wired as a half wheatstone bridge through a Vishay strain gage indicator 2120B with a bridge excitation of 1–10 V DC. Multiplier settings were set at × 200 and gain was set at 10.

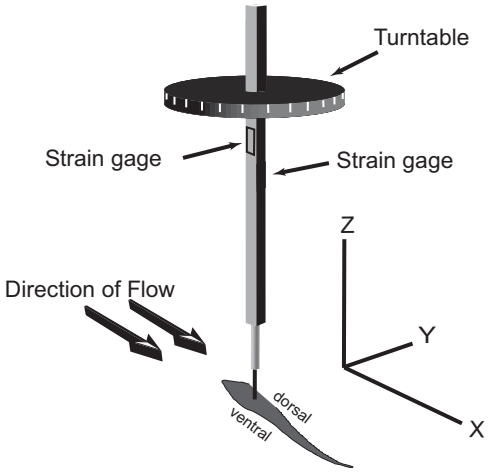


**Fig. 1.** Apparatus for varying angle of attack and measuring lift and drag in poachers postmortem. A calibrated turntable was firmly supported above the working area of the flume. The sting was fixed to the lateral surface of the euthanized fish such that the dorsoventral direction was along the *y*-axis and the mediolateral direction along the *z*-axis. At zero angle of attack (shown here), the direction of flow is along the *x*-axis, lift is along the *y*-axis and drag along the *x*-axis. Dual calibration of *x* and *y* forces allowed lift and drag to be calculated at various angles of attack set by the turntable.

When a force was applied in the *x* or *y* direction, the change in voltage was recorded. This force balance system was calibrated by loading the sting in both the *x* and *y* directions simultaneously. Voltage measurements were taken at each of 36 weight combinations ranging from 0 to 5 g on each axis. A Matlab script was written (by Emily Israeli) to determine the relationship between the known weights and voltages under dual axis loading schemes. This script first determines the relationship between the raw voltages measured versus the forces generated from the known hanging weights. The script then creates a calibration matrix for the various known weight combinations. The matrix is then used to calculate calibration coefficients based on the voltages measured and the known weights that were used. Finally, the script verifies these coefficients by comparing the force calculated by multiplying the calibration coefficient by the measured voltage to the known force. Percent error was calculated and plotted. Percent error was found to be less than 8% for the poacher force measurements. This Matlab script is available for evaluation and use (contact the corresponding author).

Voltage measurements were taken at three flow speeds, 20, 25, and 32 cm $s^{-1}$ at angles of attack ranging from 0° to 40° (in 5° increments). A calibrated turntable attached to the sting was used to vary angle of attack (Fig. 1). Slower flow speeds than 20 cm $s^{-1}$ were attempted, but these data were too noisy to be included in the analysis. Voltage data were acquired using a National Instruments data acquisition board and LabView7 (National Instruments, Austin, TX, USA) and voltage was averaged over a sampling time of 20 s for a given combination of speed and angle of attack.

### Analysis

Data were analyzed in Igor Pro 5.01 (Wavemetrics, Lake Oswego, OR, USA). Force measurements in the *x* and *y* directions were taken with respect to the fish for each angle of attack. The following equations were used to convert these measurements to lift ($L$) and drag ($D$) with respect to the flow from the component forces when the angle of attack ($\theta$) was changed:

$$L = F_x \sin(\theta) + F_y \cos(\theta)$$
$$D = F_y \sin(\theta) + F_x \cos(\theta)$$

Due to the fish being mounted on its lateral surface, lift was measured in the *y* direction and drag in the *x* direction (Fig. 1).

Correlation analysis of lift measurements at 20, 25, and 32 cm $s^{-1}$ and angle of attack was performed. As mentioned above, the force measurements were somewhat noisy, so the data were checked for outliers. Two points out of 81 lift measurements fell outside the 95% confidence ellipses. Mahalanobis distance and jackknife distance

measures confirmed these two points as outliers (95% confidence). So they were removed from the data set. Analysis of covariance, with individual as a factor, and both velocity and angle of attack as covariates, was used to determine the effects of angle of attack and swimming velocity on lift and to test for individual effects (JMP version 5.0). Least-squares regression lines were fit to the lift versus angle of attack data for each individual fish at each flow speed, and 95% confidence curves plotted.

## Results

### Kinematics

Under the laboratory conditions of the current study, *A. vulsa* was found to swim almost exclusively with its pectoral fins with a top measured speed of 28.2 cm $s^{-1}$. No pectoral–caudal gait transition was observed. Use of the caudal fin to generate thrust was only observed during escape responses. The second, more posterior, dorsal fin remained raised throughout locomotion, while the first dorsal fin was employed only during turning. The anal fin was used rarely during steady locomotion, and the caudal fin seemed to be used only for stabilization during turning and braking. Observations of seven *A. vulsa*, both during spontaneous swimming in sea tables and in our filming arena, as well as observations of four other poacher species, showed that poachers have a strong tendency to swim close to the bottom.

The pectoral fins display a sculling pattern, typical of pure labriform locomotion, moving in phase with one another in repetitive, sinusoidal cycles of abduction and adduction. The pectoral fin tip passes along a smooth

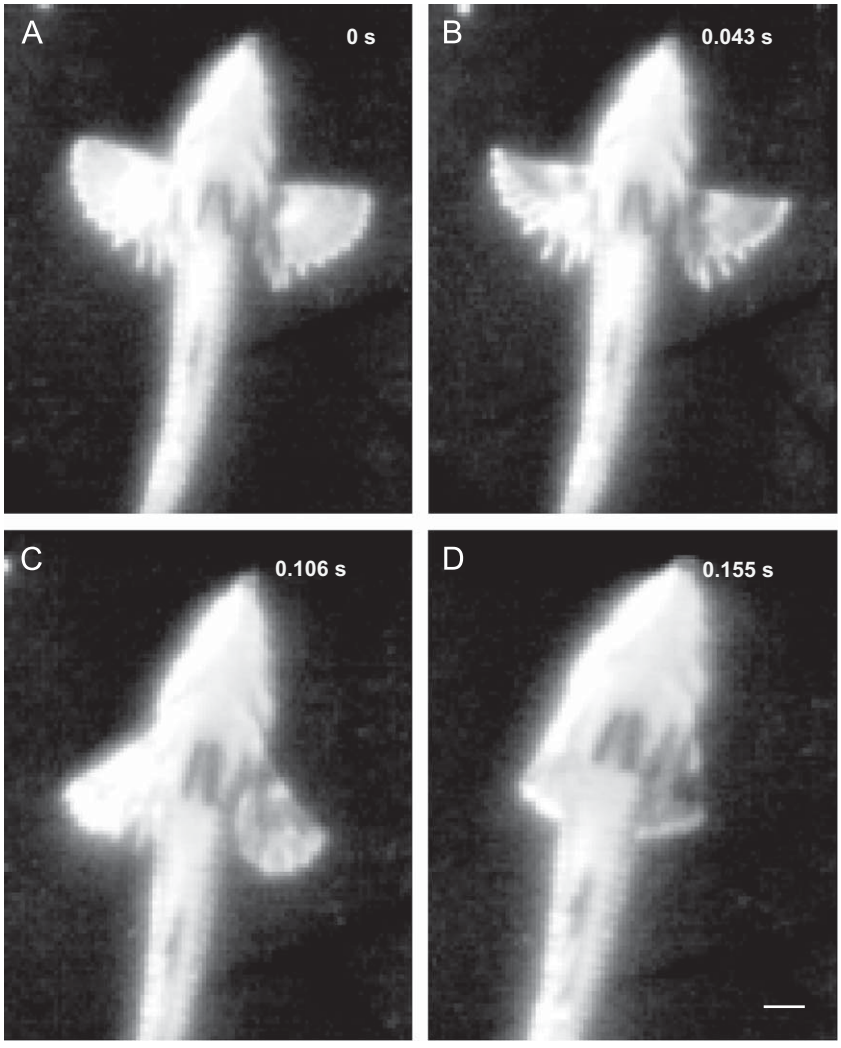


**Fig. 2.** Poacher pectoral fin stroke kinematics. (A) Pectoral fins fully abducted at the beginning of the power stroke (0 s). (B) The leading edge has curled ventrally forming a pocket (0.043 s). (C) Adduction of the pectoral fin (0.106 s). (D) Pectoral fins fully adducted against the body of the fish (0.155 s). Fish is moving from the bottom of the image toward the top of the image, and the distance traveled over the course of this fin beat cycle was 2.88 cm. Scale bar = 1 cm.

figure-eight-shaped path in the course of one cycle. As the fin begins its power stroke, the leading edge folds over forming a pocket (Fig. 2, 0.043 s). The power stroke ends with the pectoral fins adducted alongside the body of the fish (Fig. 2, 0.155 s). The leading edge then flattens back out during the recovery stroke, and the pectoral fins are held out for a period of time while the fish glides forward before moving into the next fin cycle (Fig. 2, 0 s). Observed swimming speeds ranged from 0.65 to 1.76 bl $s^{-1}$ (10.4–28.2 cm $s^{-1}$).

When swimming more than 1 cm above the bottom, poachers varied the angle of attack (i.e. pitch angle of the body) between 5° and 30° (Fig. 3A, blue symbols), but when swimming within 1 cm of the bottom, the angle of attack was consistently less than 1° (Fig. 3A, red symbols). Analysis of covariance on angle of attack, with individual and height above the bottom (high or low) as factors and body velocity as the covariate, showed an overall significance of $p<0.0001$, with significant effects of height and velocity on angle of attack ($p<0.0001$ and $p=0.014$, respectively). There was no significant effect of individual fish on angle of attack ($p=0.706$). So results from all individuals were pooled within each swimming height group for regression analysis.

When the fish swam more than 1 cm above the bottom, angles of attack showed a strong inverse relationship with overall swimming speed (Fig. 3B, blue line; $y=-0.97x+29.3$; $R^2=0.60$, $p=0.003$). As the swimming velocity increased, the angle of the body to the horizontal decreased (Fig. 3B–D). There was also a statistically significant inverse relationship between angle of attack and velocity when fish swam within 1 cm of the bottom (Fig. 3B, red line; $y=-0.04x+1.16$; $R^2=0.49$; $p=0.017$), but the absolute variation in angle was small (less than 1°).

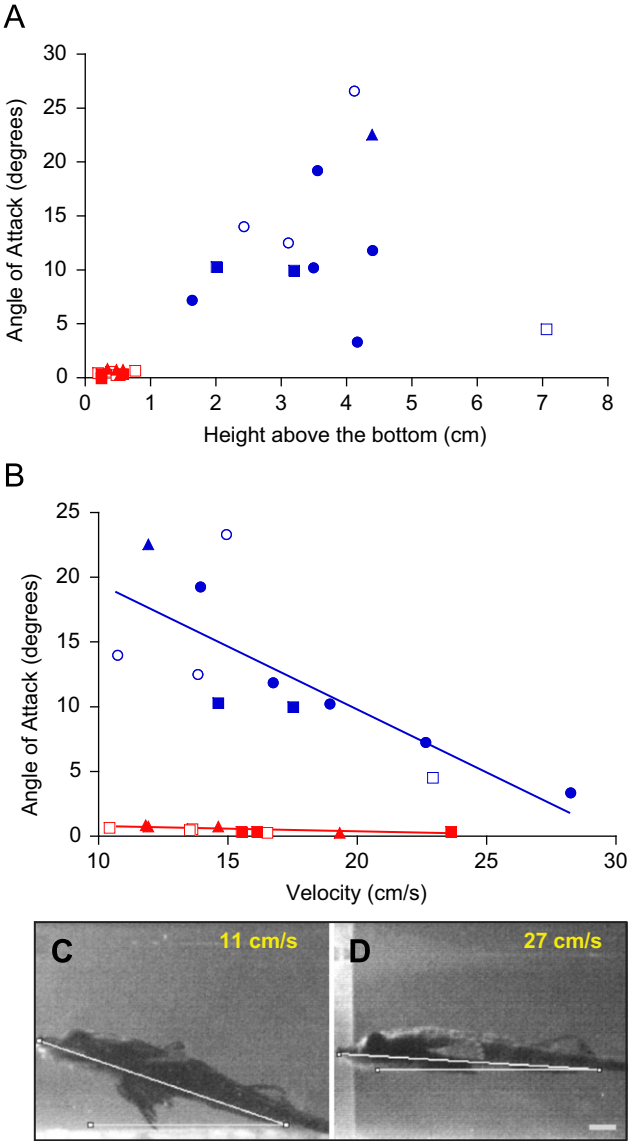


**Fig. 3.** Angle of attack (body pitch angle) for five spearnose poachers swimming freely in a large aquarium. Blue symbols indicate fish swimming more than 1 cm above the bottom and red symbols indicate fish swimming within 1 cm of the bottom. The different symbols (open circle, closed square, etc.) indicate the five different individual fish and are consistent across the red and blue groups. (A) The fish did not exhibit body pitch angles of more than 1° when swimming within 1 cm of the bottom (red symbols). Above 1 cm (blue symbols), body pitch angles ranged from 5° to 30°. (B) When more than 1 cm above the bottom, fish select substantially higher angles of attack when they swim slowly (blue line). When within 1 cm of the bottom, fish also select higher angles of attack when swimming slowly, but the absolute change in angle is small. (C) Frame from a video of a poacher swimming at a low velocity with a high angle of attack. (D) Frame from a video of a poacher swimming at a high velocity with a low angle of attack. Scale bar = 1 cm.

### Support of body weight when swimming in the water column

As described above, when poachers swim 1 cm or more above the bottom, the angle of attack of the body increases with a decrease in swimming velocity (Fig. 3B). To determine the amount of lift generated by the body alone, the pectoral fins were removed from three specimens postmortem and lift and drag were measured at three flow speeds (20, 25, and 32 cm $s^{-1}$) over a range of body pitch angles (0–40°) in a flume.

As expected, lift measurements indicate that as the angle of attack increases, lift generation at a given flow speed increases (Fig. 4A). Combined ANCOVA on lift from three fish at three flow speeds and nine body pitch angles per speed showed significant effects of increasing flow velocity and angle of attack on lift ($p<0.0001$ for both effects), and also a significant effect of individual fish ($p=0.016$). Drag also increases with increasing angle of attack (Fig. 4B), with statistically significant effects of flow velocity, angle of attack and individual on drag ($p<0.0001$, $p<0.0001$, and $p=0.009$, respectively).

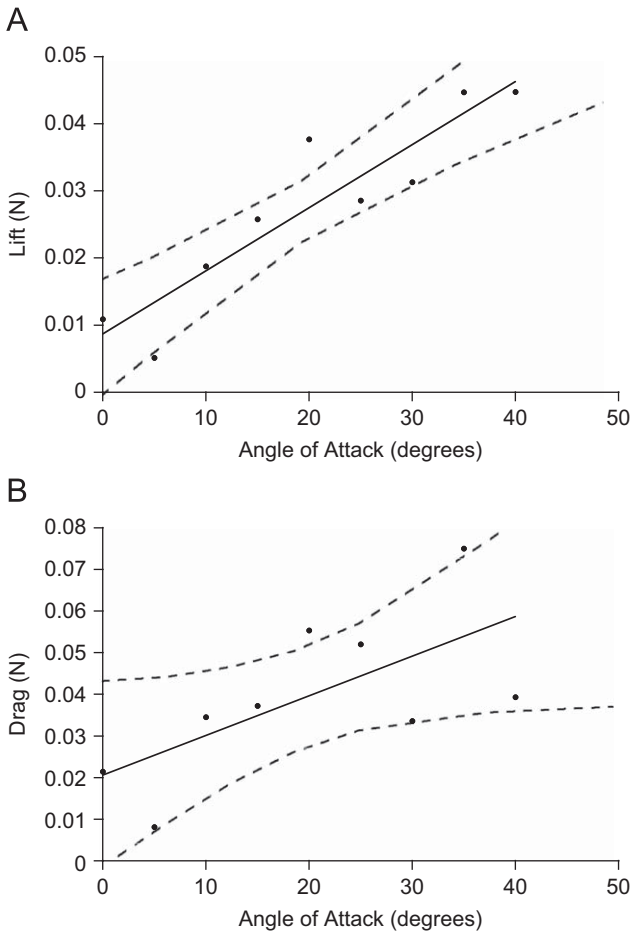


**Fig. 4.** Lift and drag measured postmortem on specimens with pectoral fins removed. These are example plots of lift and drag versus angle of attack for one individual fish at a flow speed of 25 cm/s, with least-square regression lines and 95% confidence interval curves. (A) Lift versus angle of attack (from individual 03; $R^2 = 0.85$; $p = 0.001$). (B) Drag versus angle of attack (from individual 03; $R^2 = 0.45$; $p = 0.050$).

The finding of significant individual effects makes pooling the lift data from the three individual fish inappropriate. Therefore, to quantify the lift force, least-squares regression was used to fit lines and confidence curves to the lift curves for the three individual fish at 20 and 25 cm $s^{-1}$ (32 cm $s^{-1}$was not used because it is beyond the range of speeds measured *in vivo*; Fig. 3B). At 20 cm $s^{-1}$, the biologically relevant angle of attack is 10°, and at 25 cm $s^{-1}$it is 5° (from Fig. 3B). One of three regressions at 20 cm $s^{-1}$was not significant ($p = 0.102$). For the remaining two, the lift force at 10° angle of attack was calculated from the regression equations and the 95% confidence intervals read from the confidence curves, yielding $7.4 \pm 2.5$ mN ($p = 0.017$) for individual 01 and $11.7 \pm 7.5$ mN ($p = 0.013$) for individual 02. At 25 cm $s^{-1}$and 10°, lift forces were $9.4 \pm 10.5$ mN ($p = 0.014$), $16.1 \pm 11.0$ mN ($p = 0.013$), and $13.4 \pm 7.5$ mN ($p = 0.001$) for the three individuals, respectively. For comparison, the weights in water of the three fish were 19.9, 21.9, and 24.0 mN, respectively.

Qualitative visualization of fluid streaklines was used to study the hydrodynamics of the pectoral fins. Fig. 5A

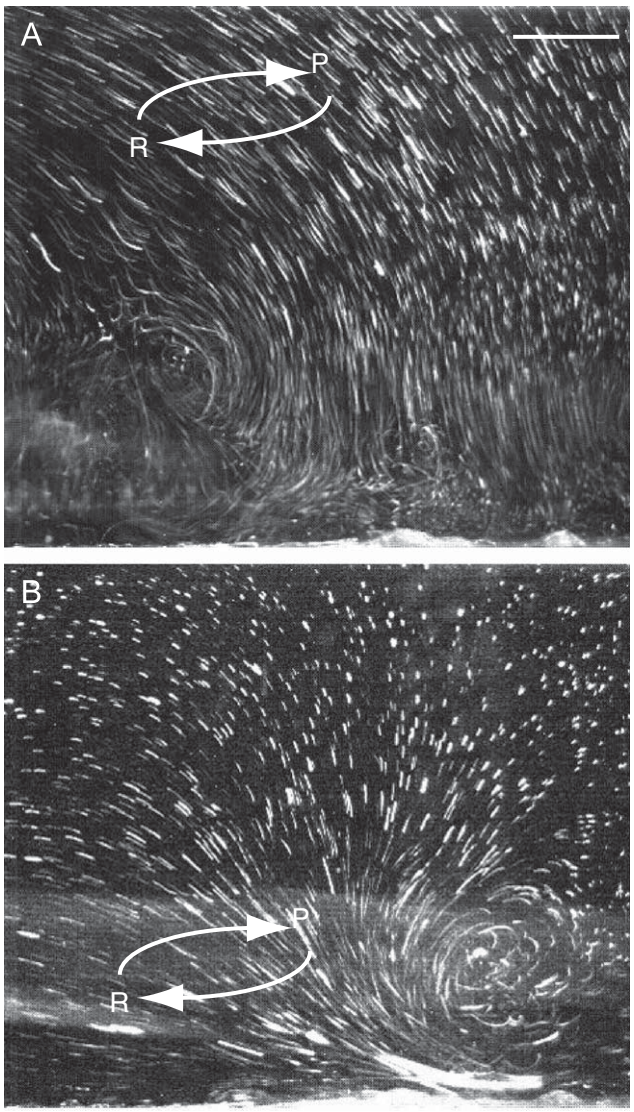


**Fig. 5.** Lateral view of streaklines showing the wake from a pectoral fin power stroke (A) more than 1 cm above the bottom and (B) within 1 cm of the bottom. The fish is no longer in the field of view. Arrows indicate a schematic of the path of the pectoral fin during the power stroke (*P*) and recovery stroke (*R*) that occurred previously. Particle displacements were averaged over 0.36 s. The fish has traveled from right to left in both images, passing its pectoral fin through the plane of the laser. Above 1 cm in the water column (A), the streaklines show relatively little interaction of the flow with the bottom of the aquarium. Within 1 cm of the bottom (B), the wake is much more organized. Fluid is being pulled down from above and pushed posteriorly and ventrally resulting in a vortex that can be seen interacting with the ground in the lower right-hand corner of the image. The bright streak is a result of the neutrally buoyant, illuminated particles coming into contact with the bottom of the aquarium. Scale bar = 1 cm.

shows streaklines rendered from a video of a poacher swimming more than 1 cm above the bottom. The streaklines show relatively little interaction of the flow with the floor of the aquarium (compared with Fig. 5B when swimming within 1 cm of the bottom). In the two other analyzed sequences of fish swimming more than 1 cm above the bottom, the observed pectoral fin wakes were qualitatively similar to Fig. 5A.

### Support of body weight when swimming along the bottom

When swimming within 1 cm of the bottom, poachers select a mean body pitch angle of just 0.41° (Fig. 3B), indicating lower lift forces on the body than when the fish is above 1 cm in the water column where it can select higher angles of attack (Figs. 3A and 4A).

Within 1 cm of the bottom, the resulting wake from the pectoral fins is more organized than that of the fish swimming above 1 cm in the water column (Fig. 5B). Fluid is drawn from above the fish and pushed posteriorly and ventrally creating a counterclockwise vortex in the bottom right-hand corner of the image. The bright white line along the bottom of the image shows the vortex interacting strongly with the floor of the aquarium. This line is a result of the neutrally buoyant particles that have been illuminated by the sheet of laser coming into contact with the bottom. In the five other analyzed sequences of fish swimming within 1 cm of the bottom, the observed pectoral fin wakes were qualitatively similar to Fig. 5B.

### Advance ratio

Advance ratios were calculated for all sequences from all five fish divided between sequences of swimming along the bottom and more than 1 cm above the bottom (Fig. 6). Analysis of covariance showed a significant direct relationship between advance ratio and velocity ($p < 0.0001$). Fish swimming near the bottom showed statistically significantly higher advance ratios ($p = 0.047$), although the magnitude of the difference was fairly small (Fig. 6). No significant effect of individual on advance ratio was found ($p = 0.604$).

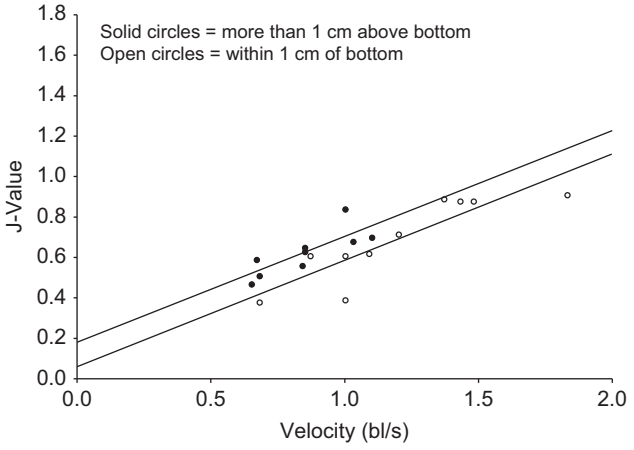


**Fig. 6.** Advance ratio ($J$) for all recorded swimming sequences from five fish. Advance ratio increases with increased swimming speed ($p < 0.0001$), and advance ratio is higher when the fish swim within 1 cm of the bottom ($p < 0.047$), indicating greater mechanical efficiency.

## Discussion

The northern spearnose poacher, *A. vulsa*, uses different strategies for counteracting negative buoyancy depending on whether the fish is swimming in the water column or within 1 cm of the bottom. In the water column, it swims with a high body pitch angle (5–20°), and lift from the body surface alone supports approximately half of its weight in water (Figs. 3 and 4).

When the fish swim very close to the bottom, however, they cannot pitch the body up and still keep the center of mass within 1 cm of the bottom. This constraint suggests that poachers should not be able to swim slowly when near the ocean floor because they cannot increase angle of attack and generate enough lift to keep from sinking to the bottom. Nonetheless, we see in Fig. 3B that poachers are able to swim with the same range of speeds along the bottom as they do in the water column. Therefore, another mechanism must be in use. Qualitative flow visualization with particle streaklines suggests that fish swimming close to the bottom rely on a hydrodynamic ground effect in which vortices generated by the pectoral fins interact with the substrate to augment lift and counteract negative buoyancy (Fig. 5B).

When swimming more than 1 cm above the bottom, the spearnose poacher employs a positive body pitch angle that decreases with increasing swimming speed (Fig. 3B). Since lift increases with flow speed, the decreasing body pitch angle suggests that the fish are adjusting their posture such that lift generation from the body surface remains approximately constant at different combinations of swimming speed and angle of attack. The postmortem lift measurements support this conclusion, showing that approximately half of the weight in water is supported by lift from the body surface at the biologically relevant combinations of 20 cm $s^{-1}$and 10° and 25 cm $s^{-1}$and 5°. However, the lift measurements were noisy, as indicated by the wide 95% confidence curves on the regressions of lift versus angle of attack (Fig. 4A). Thus we have fairly low confidence in the exact lift force values reported here, but based on the five values and their confidence intervals, we do feel confident that roughly half of the spearnose poacher's weight in water is supported by body lift when the fish are swimming more than 1 cm above the bottom.

When the poacher body pitch angles are compared to those of other negatively buoyant fish, the angles of

attack for the spearnose poacher tend to be higher. At a swimming velocity of 0.5 bl/s, white sturgeons, leopard sharks, and Atlantic mackerels exhibit body pitch angles of 20°, 11°, and 9°, respectively, whereas the angle for *A. vulsa* is 22°. When swimming velocity increases to 1.0 bl/s, angle of attack of the body decreases to 14° for the poachers, 9° for white sturgeons, 8° for leopard sharks, and 0° for Atlantic mackerels (He and Wardle, 1986; Wilga and Lauder, 1999, 2000). It is possible that the higher angles of attack exhibited by the spearnose poacher, relative to other species, may be caused by greater density resulting from the body armor of these fish.

Decreasing angle of attack with increasing swimming speed keeps lift approximately constant and also would be expected to reduce drag at higher speeds. Our postmortem drag measurements on spearnose poachers indicate that, as expected, drag increases with increasing flow speed and angle of attack (Fig. 4B). A behavioral strategy of reducing angle of attack would keep drag from increasing as rapidly as would be expected for a given increase in swimming speed.

It is possible that lift from the poachers' body may actually be greater than that measured from postmortem specimens in this study. Increasing the camber of an airfoil can substantially increase lift (Mueller, 2001), and observation of *A. vulsa* swimming suggests that the fish may be generating more lift by introducing camber into its body form. When swimming more than 1 cm above the bottom, the poacher sometimes curves its tail down towards the ground, introducing a slight concavity to its ventral surface. The effect of body camber was not mimicked in the postmortem specimens during the lift measurements. Lift from the pectoral fin stroke, increased camber of the body, or a combination of the two may be supplying the remaining lift above the body lift force required when fish swim more than 1 cm above the bottom.

Within 1 cm of the bottom, the poacher relies less on body pitch angle to generate lift, and presumably relies more on the fluid flow generated by the pectoral fin stroke. Fig. 5B shows the wake from the pectoral fin of a poacher swimming within 1 cm of the bottom. The counterclockwise vortex seen in the lower right-hand corner creates an equal and opposite reaction force anteriorly and dorsally, with relation to the fish. Qualitatively, these streaklines portray a vortex interacting with the ground and generating both lift and thrust. Thus, the spearnose poacher appears to be taking advantage of ground effect to augment pectoral fin lift and thrust. It is also possible that ground effect may enhance the lift generated by the body, and the spearnose poacher's ability to skim along within 1 cm of the bottom could be due to ground effect enhancement of both pectoral fin and body lift.

The use of ground effect has been studied in birds (Spedding, 1987; Rayner, 1991) and fish (Arnold and Weihs, 1978; Vogel, 1981; Webb, 2002), and has been shown to impact hydrodynamic forces significantly. When a wing, or hydrofoil, is in ground effect, fluid is constrained between the wing and the substrate causing decrease in fluid velocity below the wing (Zierhan and Zhang, 2000). The closer the hydrofoil comes to the ground, the greater the relative flow speed over the top of the wing, thereby increasing net circulation and lift.

Blake (1979) showed that while the pectoral fin kinematics of hovering mandarin fish remain relatively similar at various heights in the water column, the fish gains 30–60% savings in power due to ground effect when hovering close to the bottom. Plaice have been shown to use their proximity to the ocean floor to decrease power costs and increase lift by assuming a positive angle of attack of the body (Webb, 2002). Similar findings have been published describing a decrease in total power required for flight in a skimming bird due to ground effect (Withers and Timko, 1977). The spearnose poacher appears to be generating increases in lift and thrust by using its proximity to the ocean floor to take advantage of this same ground effect, allowing the fish to swim along the bottom of the aquarium, yet remain suspended in the water without substantially increasing its angle of attack.

The poacher's drag-based rowing may be more accurately compared to helicopter flight than to a lift-based airplane model. It has been shown that a helicopter flying in ground effect, both during hovering and forward flight at moderate speeds, experiences a significant increase in thrust and a substantial decrease in power requirements. This allows the helicopter to fly at a higher gross weight, or density altitude, than would be possible out of ground effect (Leishman, 2006). These changes in aerodynamic thrust are accompanied by counterclockwise vortices shed from the rotor tips that interact with the ground. The poacher's mechanism within 1 cm of the bottom seems to follow this same idea of generating more hydrodynamic force with a lower power requirement (Figs. 5B and 6).

This leads us to question, what, if any, are the locomotor advantages to swimming with paired fin locomotion near a substrate? The fluid flow shown in Fig. 5B indicates that the poacher is able to use the ground to augment its lift and thrust. In addition, the mechanical efficiency of the pectoral fins increases as the fish approaches the bottom (Fig. 6). Advance ratio has a similar slope relative to speed at all heights in the water column; however, along the bottom (red line) the $y$-intercept is higher ($p = 0.0465$). Moreover, it has been shown that swimming or flying in close proximity to a substrate decreases drag (Vogel, 1981). This decrease in drag would add to the increase in locomotor efficiency for a benthic fish. Therefore, for poachers, paired fin

locomotion, while sustainable above 1 cm in the water column, is more hydrodynamically efficient in close proximity to the bottom.

Thrust and lift augmentation due to proximity to the ocean floor and exploiting the body as a hydrofoil are two ways in which *A. vulsa* specializes as a negatively buoyant, labriform, benthic species. These mechanisms of generating hydrodynamic forces may have allowed poachers to develop elaborate body armor and camouflage to increase predation and predator evasion performance without sacrificing mechanical efficiency of locomotion.

## Acknowledgments

We would like to thank Nicholas Gidmark, Cally Harper, Dr. Lara Ferry-Graham, Erin Winters-Mist, Joseph Bahlman, Dr. Tonia Hsieh, Dr. Emanuel Azizi, Dr. Thomas Roberts, Dr. David Willis, Dr. Stephen Gatesy, Dr. Daniel Riskin, Dr. Gregory Sawicki, Dr. Jose Iriarte-Diaz, and all the students in the 565 fish course for their help, advice, insight, and support. We would like to thank Emily Israeli for the Matlab code used in the flume measurements. We would also like to thank Friday Harbor Laboratories for their wonderful facilities and hospitality. In addition, we would like to thank the two anonymous reviewers for their helpful comments and insight. This work was supported in part by the US National Science Foundation under Grant No. 0629372 to ELB, and by a Bushnell Graduate Research Grant to BNN.

## References

Aleev, Y.G., 1969. Function and Gross Morphology in Fish. Keter Press, Jerusalem (translated from Russian).

Arnold, G.P., Weihs, D., 1978. The hydrodynamics of rheotaxis in the plaice (*Pleuronectes platessa* L.). J. Exp. Biol. 75, 147–169.

Blake, R.W., 1979. The energetics of hovering in the mandarin fish (*Synchropus picturatus*). J. Exp. Biol. 82, 25–33.

Blake, R.W., 1983. Median and paired fin propulsion. In: Webb, P.W., Wells, D. (Eds.), Fish Biomechanics. Praeger Publishers, New York, pp. 214–247.

Bozkurttas, M., Dong, H., Mittal, R., Madden, P., Lauder, G.V., 2006. Hydrodynamic performance of deformable fish fins and flapping foils. American Institute of Aeronautics and Astronautics, AIAA 2006-1392, 1–11.

Breder Jr., C.M., 1926. The locomotion of fishes. Zoologica 4, 159–297.

Drucker, E.G., Jensen, J.S., 1996. Pectoral fin locomotion in the striped surfperch. I. Kinematic effects of swimming speed and body size. J. Exp. Biol. 199, 2235–2242.

Drucker, E.G., Lauder, G.V., 2000. A hydrodynamic analysis of fish swimming speed: wake structure and locomotor force in slow and fast labriform swimmers. J. Exp. Biol. 203, 2379–2393.

He, P., Wardle, C.S., 1986. Tilting behavior of the Atlantic mackerel, *Scomber scombrus*, at low swimming speeds. J. Fish Biol. 29, 223–232.

Leishman, J.G., 2006. Principles of Helicopter Flight. Cambridge University Press, New York.

Mueller, T.J., 2001. Fixed and Flapping Wing Aerodynamics for Micro Air Vehicle Applications. American Institute of Aeronautics and Astronautics, Inc., Reston, VA, USA.

Mussi, M., Summers, A.P., Domenici, P., 2002. Gait transition speed, pectoral fin-beat frequency and amplitude in *Cymatogaster aggregata*, *Embiotoca lateralis*, and *Damalichthys vacca*. J. Fish Biol. 61, 1282–1294.

Nelson, J.S., 1994. Fishes of the World, third ed. Wiley, New York.

Rayner, J.M.V., 1991. On the aerodynamics of animal flight in ground effect. Phil. Trans. R. Soc. B 334, 119–128.

Spedding, G.R., 1987. The wake of a kestral (*Falco tinnunculus*) in gliding flight. J. Exp. Biol. 127, 45–57.

Vogel, S., 1981. Life in Moving Fluids. Princeton University Press, Princeton.

Walker, J.A., Westneat, M.W., 1997. Labriform propulsion in fishes: kinematics of flapping aquatic flight in the bird wrasse *Gomphosus varius* (Labridae). J. Exp. Biol. 200, 1549–1569.

Walker, J.A., Westneat, M.W., 2001. Performance limits of labriform propulsion and correlates with fin shape and motion. J. Exp. Biol. 205, 177–187.

Webb, P.W., 2002. Kinematics of plaice, *Pleuronectes platessa*, and cod, *Gadus morhua*, swimming near the bottom. J. Exp. Biol. 205, 2125–2134.

Wilga, C.D., Lauder, G.V., 1999. Locomotion in sturgeon: function of the pectoral fins. J. Exp. Biol. 202, 2413–2432.

Wilga, C.D., Lauder, G.V., 2000. Three-dimensional kinematics and wake structure of the pectoral fins during locomotion in leopard sharks *Triakis semifasciata*. J. Exp. Biol. 203, 2261–2278.

Wilga, C.D., Lauder, G.V., 2001. Functional morphology of the pectoral fins in bamboo sharks, *Chiloscyllium plagiosum*: benthic versus pelagic station-holding. J. Morphol. 249, 195–209.

Withers, P.C., Timko, P.L., 1977. The significance of ground effect to the aerodynamic cost of flight and energetics of the black skimmer (*Rhyncops nigra*). J. Exp. Biol. 70, 13–26.

Zierhan, J., Zhang, X., 2000. Aerodynamics of a single element wing-in-ground effect. J. Aircraft 37, 1058–1064.